Proceedings of the Seventeenth (2007) International Offshore and Polar Engineering Conference
Lisbon, Portugal, July 1-6, 2007

ISBN 978-1-880653-68-5; ISBN 1-880653-68-0(Set); ISSN 1098-6189 (Set)

A Refined Model for Float Type Energy Conversion Device

Kesayoshi Hadano[(1)], Pallav Koirala[(2)], Kimihiko Nakano[(3)],Kunihiro Ikegami[(4)]
(1), (2) School of Science and Engineering, Yamaguchi University, Ube, Yamaguchi, Japan
(3) Institute of Industrial Science, University of Tokyo, Tokyo, Japan
(4) Dept. of Naval Architecture, Nagasaki Institute of Applied Science, Nagasaki, Japan

ABSTRACT

A refined dynamics model for the float-counterweight wave energy conversion system is presented here taking into account the previously unconsidered effects of the added mass and drag force on the behavior of float motion and energy gain. Computational results of the work rate, where the float was always in a partially submerged state were found to be in good agreement with the results obtained from wave tank tests. Comparative analysis of the results from the new and previous model has led to a better understanding of the effects of added mass and drag force on the system. Resonant frequency and the power output during resonance have been calculated for certain prototype designs.

KEY WORDS: Resonant heaving motion; driving pulley; wire tensile force; float; counterweight.

INTRODUCTION

The importance of wave energy conversion need not be exaggerated especially in the context of today's global environment which faces the problem of a massive increase in energy demand coupled with a rise in global warming. Various mechanisms for extracting wave energy have been developed but have not been fully utilized due to structural strength and economical problems. The OWC system seems to be considered a major one because it does not have serious problems of structural strength (Evans et. al. 1982, Malmo et. al. 1985, Folley et. al 2004, Suzuki et. al. 2006). However its practical use has not been attained due to economical reasons.
The authors have proposed a movable body type in which the heaving motion of the partially submerged float causes the driving pulley and the shaft to rotate as shown in Fig. 1.The rotary converter rotates the shaft in a single direction independent of the direction of the float motion, i.e. up or down. The gearbox increases output shaft speed so that the size of the generator can be reduced depending upon the gear ratio. The vertical motion of the float and therefore the energy gain is maximum during resonance, which will be discussed later. Therefore, the system can be designed so that its natural frequency of oscillation matches that of the dominant wave frequency which will enable us to reduce the component sizes for a given energy output. The use of wire, made with a flexible material frees the system from serious structural problems common to most movable body type systems. Since all mechanical and electrical components except the float and the counterweight are set well above the water level, their supervision and maintenance is convenient. As a remaining problem, since the float on the water surface will trace an elliptical orbit in the wave field, a horizontal force will act on the float and therefore on the system. To obviate this problem and enhance the vertical motion of the float, the device can be located in slit type caissons as shown in Fig. 2.
Drag and added mass forces impede the motion of the float mass in water. Hadano (1998) proposed a dynamics model for the system where these forces had not been considered. This paper aims to propose a refined model considering all these forces, with an objective of understanding the dynamics of the system in the real environment. Computational results of the time series of various physical quantities have been presented using the new model highlighting the effects of the drag and added mass force. Next, the resonance phenomenon and its utilization in enhancing the energy extraction have been discussed.

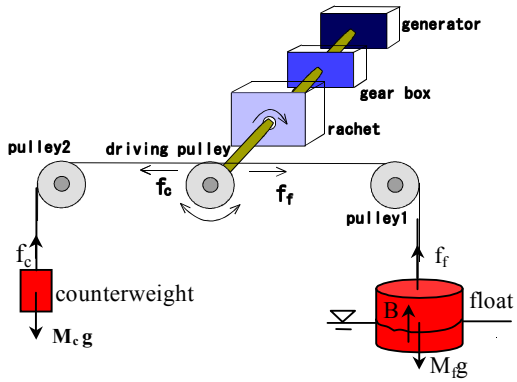

Fig. 1 Schematic diagram of the energy conversion system

THE MECHANICAL DYNAMICS MODEL

As shown in Fig.1, the device consists mainly of a float, counterweight, cable, driving pulley, ratchet, gearbox and generator. The mechanism of energy transfer is basically the conversion of the heaving of the float

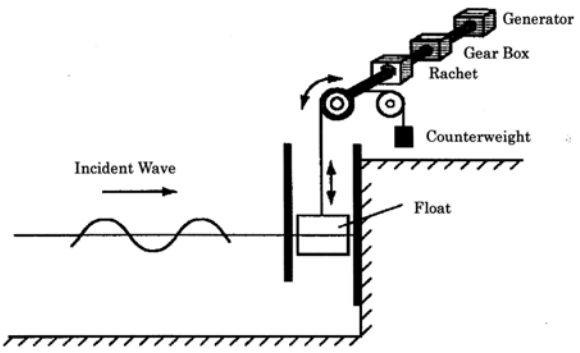

Fig. 2 Float set in a caisson to prevent its horizontal swaying

mass into a rotational motion of the shaft connected to the electric generator. The ratchet mechanism converts the bi-directional rotation of the driving pulley into a unidirectional rotation of the shaft which is then accelerated by the gearbox. In principle the system can extract energy both when the float is moving up and down corresponding to the rise and fall of the water level. But as the weight of the counterweight is much less than that of the float, it does not generate enough torque to rotate the driving pulley when the water level is rising. This causes the cable on the float side to slacken. As a result of this, the cable experiences a sudden unsafe tensile force due to the weight of the float when the water level falls. Therefore we devised the rotary converter so that the generator works only when the float is falling. Data for energy gain presented in this paper are also only for the case when the float is falling.

EQUATIONS FOR THE DYNAMICS MODEL

In this section, a mathematical model of the physical process of energy conversion has been discussed. It is noted here that the model takes into account only the vertical motion of the float. The motion of the float in other directions has not been included since the authors are interested in studying the dynamics of the system shown in Fig. 2, where the caisson walls prevent the horizontal force of the wave reaching the float.

Equations for the Generator

If θ is the angle of rotation of the driving pulley in anticlockwise direction, the torque that the driving pulley receives from the generator in anticlockwise direction, τ, and the potential difference between the two terminals of the generator, e, are given by Eq. 1 and Eq. 2 respectively.

$$\tau = -Gk_\tau i \cdot \mathrm{sgn}(\dot{\theta}) \tag{1}$$

$$e = Gk_e \dot{\theta} \cdot \mathrm{sgn}(\dot{\theta}) \tag{2}$$

where, $\dot{\theta}$ is the angular velocity of the driving pulley, i is the current flowing in the coil of the generator, sgn(x) =1 for x>0 and –1 for x<0, G is the total gear ratio from the driving pulley to the generator, k_τ is the torque constant, k_e is the induced voltage constant. Here the effect of the ratchet mechanism is ignored and the minus sign in Eq. 1 indicates that the driving pulley receives an anticlockwise torque from the generator when the float is falling and vice versa.

Force Balance at Stationary Free State

The left part of Fig. 3 shows the instance of float and water surface at stationary condition without work, and the right part of the figure shows their situation at an arbitrary time when the system is working. Eq. 3 gives the equilibrium equation of the force for the circular cylindrical float chosen for this work in a stationary condition.

$$M_c g + \frac{1}{4}\pi d_f^2 \rho_w h g = M_f g \tag{3}$$

where, M_f: mass of the float, M_c: mass of the counterweight, d_f: diameter of the float, h: submerged height of the float, ρ_w: density of water.

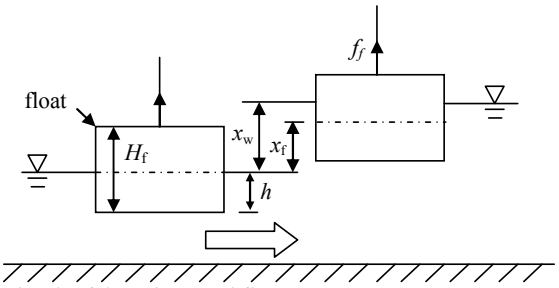

Fig. 3 Sketch of the submerged float

Equations for the Heaving Motion of the Float

When heaving, the float can be found in three different states of submergence depending on the height and the time period of the wave, which are listed below along with the appropriate equations of motion.

(1) Float is partially submerged $(0 \le h + x_w - x_f \le H_f)$

$$M_f \frac{d^2x_f}{dt^2} = f_f + \frac{1}{4}\pi d_f^2 \rho_w (h + x_w - x_f) g - M_f g + \frac{1}{8} C_d \rho_w \left| \frac{dx_w}{dt} - \frac{dx_f}{dt} \right| \left(\frac{dx_w}{dt} - \frac{dx_f}{dt} \right) \pi d_f^2 - \frac{1}{4} C_m \pi d_f^2 \rho_w \left(h + x_w - x_f \right) \frac{d^2x_f}{dt^2} \tag{4}$$

(2) Float is wholly submerged $(h + x_w - x_f > H_f)$

$$M_f \frac{d^2x_f}{dt^2} = f_f + \frac{1}{4}\pi d_f^2 \rho_w H_f g - M_f g + \frac{1}{8} C_d \rho_w \left| \frac{dx_w}{dt} - \frac{dx_f}{dt} \right| \left(\frac{dx_w}{dt} - \frac{dx_f}{dt} \right) \pi d_f^2 - \frac{1}{4} C_m \pi d_f^2 \rho_w H_f \frac{d^2x_f}{dt^2} \tag{5}$$

(3) Float is hung in the air $(h + x_w - x_f < 0)$

$$M_f \frac{d^2x_f}{dt^2} = f_f - M_f g \tag{6}$$

In Eqs. 4~6, H_f: height of the float, C_d: drag coefficient, C_m: coefficient of added mass, f_f: tensile force in the cable supporting the float, x_f and x_w: displacements of the float and water level respectively measured upward from the stationary free state as shown in Fig. 3.

The drag force used in the above equations is defined as

$$F_D = \frac{1}{2} \rho_w C_d v_r |v_r| \tag{7}$$

where v_r is the relative velocity between the vertical velocity of water and the float.

The force due to the added mass is defined as

$$F_M = \rho_w C_m \overline{V} \alpha \tag{8}$$

where $\overline{V}$ is the submerged volume and α is the vertical acceleration of the float.

Since the float is cylindrical in shape, we assume the added mass equal to the mass of the volume of water displaced by the float in motion. Therefore the added mass will not remain constant but depend on the relative displacement of the water level and float as indicated in Eqs. 4~5. The added mass force and the drag force both oppose the motion of the float in water and therefore appear only in the first two states, mentioned above as (1) and (2), of the float submergences.

Equations for the Driving Pulley Motion

The equation of the rotation of the driving pulley is as follows

$$I\frac{d^2\theta}{dt^2}+C\frac{d\theta}{dt}=\tau+(f_c-f_f)R_m \tag{9}$$

where, I : the mass moment of inertia of rotating bodies, C : viscous damping coefficient, R_m : radius of driving pulley, f_c: tensile force of the wire supporting the counterweight evaluated from Eq. 10.

$$f_c=M_c(g+\ddot{x}_c) \tag{10}$$

where, $(\ddot{x}_c)$ is the acceleration of the counterweight.

Eliminating the wire tensile force, f_f, from Eq. 9 using Eqs. 4~6, we obtain the following equations.

(1) Float is partially submerged $(0\le h+x_w-x_f\le H_f)$

$$I\frac{d^2\theta}{dt^2}+C\frac{d\theta}{dt}=\tau+f_cR_m+\left(\frac{\rho g\pi}{4}d_f^2(h+x_w-x_f)-M_fg-M_f\frac{d^2x_f}{dt^2}\right)R_m+ \tag{11}$$
$$\left(\frac{1}{8}C_d\rho_w\left|\frac{dx_w}{dt}-\frac{dx_f}{dt}\right|\left(\frac{dx_w}{dt}-\frac{dx_f}{dt}\right)\pi d_f^2-\frac{1}{4}C_md_f^2\rho_w(h+x_w-x_f)\frac{d^2x_f}{dt^2}\right)R_m$$

(2) Float is wholly submerged $(h+x_w-x_f>H_f)$

$$I\frac{d^2\theta}{dt^2}+C\frac{d\theta}{dt}=\tau+f_cR_m+\left(\frac{\rho g\pi}{4}d_f^2H_f-M_fg-M_f\frac{d^2x_f}{dt^2}\right)R_m+ \tag{12}$$
$$\left(\frac{1}{8}C_d\rho_w\left|\frac{dx_w}{dt}-\frac{dx_f}{dt}\right|\left(\frac{dx_w}{dt}-\frac{dx_f}{dt}\right)\pi d_f^2-\frac{1}{4}C_md_f^2\rho_wH_f\frac{d^2x_f}{dt^2}\right)R_m$$

(3) Float is hung in the air $(h+x_w-x_f<0)$

$$I\frac{d^2\theta}{dt^2}+C\frac{d\theta}{dt}=\tau+f_cR_m-\left(M_fg+M_f\frac{d^2x_f}{dt^2}\right)R_m \tag{13}$$

Since the cable is fixed at a point on the driving pulley and wound around it, the displacement of the float and the angle of rotation of the pulley can be written as follows

$$x_f=R_m\theta \tag{14}$$

Eq. 1 and Eq. 2 can be combined to write the torque as follows

$$\tau=-\frac{G^2}{r}k_tk_e\frac{d\theta}{dt} \tag{15}$$

where, the expression $e=i\cdot r$ is applied; in which r is the internal resistance of the generator.

Using Eqs. 14~15 in Eqs. 11~13, the following second order differential equations are obtained for the angle of rotation of the driving pulley.

(1) Float is partially submerged $(0\le h+x_w-x_f\le H_f)$

$$\left(\frac{I}{R_m}+(M_f+M_c)R_m+\frac{\rho_w\pi d_f^2C_m}{4}(h+x_w-R_m\theta)R_m\right)\frac{d^2\theta}{dt^2}+\frac{1}{R_m}\left(C+\frac{G^2k_tk_e}{r}\right)\frac{d\theta}{dt}+ \tag{16}$$
$$\frac{\rho_wg\pi}{4}d_f^2R_m\theta=\frac{\rho_wg\pi}{4}d_f^2x_w+\frac{1}{8}\rho_w\pi C_dd_f^2\left|\frac{dx_w}{dt}-R_m\frac{d\theta}{dt}\right|\left(\frac{dx_w}{dt}-R_m\frac{d\theta}{dt}\right)$$

Previous model

$$\left(\frac{I}{R_m}+(M_c+M_f)R_m\right)\frac{d^2\theta}{dt^2}+\frac{1}{R_m}\cdot\left(C+\frac{G^2}{r}k_tk_e\right)\frac{d\theta}{dt}+\frac{\rho_wg\pi}{4}d_f^2R_m\theta=\tau+\frac{\rho_wg\pi}{4}d_f^2x_w$$

(2) Float is wholly submerged $(h+x_w-x_f>H_f)$

$$\left(\frac{I}{R_m}+(M_c+M_f)R_m+\frac{\rho_w\pi C_md_f^2H_f}{4}R_m\right)\frac{d^2\theta}{dt^2}+\frac{1}{R_m}\cdot\left(C+\frac{G^2}{r}k_tk_e\right)\frac{d\theta}{dt}=$$
$$=\frac{\rho_wg\pi}{4}d_f^2H_f+(M_c-M_f)g+\frac{1}{8}\rho_w\pi C_dd_f^2\left|\frac{dx_w}{dt}-R_m\frac{d\theta}{dt}\right|\left(\frac{dx_w}{dt}-R_m\frac{d\theta}{dt}\right) \tag{17}$$

Previous model

$$\left(\frac{I}{R_m}+(M_c+M_f)R_m\right)\frac{d^2\theta}{dt^2}+\frac{1}{R_m}\cdot\left(C+\frac{G^2}{r}k_tk_e\right)\frac{d\theta}{dt}=\frac{\rho_wg\pi}{4}d_f^2H_f+(M_c-M_f)g$$

(3) Float is hung in the air $(h+x_w-x_f<0)$

$$\left(\frac{I}{R_m}+(M_c+M_f)R_m^2\right)\frac{d^2\theta}{dt^2}+\frac{1}{R_m}\cdot\left(C+\frac{G^2}{r}k_tk_e\right)\frac{d\theta}{dt}=(M_c-M_f)g \tag{18}$$

Eqs. 16~18 can be solved numerically to obtain the time series of θ and $\dot{\theta}$ and hence the wire tensile force, torque and displacement of the float can be evaluated. The output power is calculated from the following equation.

$$P_G=r\cdot i^2=r\left(\frac{-Gk_e}{r}\dot{\theta}\right)^2 \tag{19}$$

Calculation Conditions

As represented by Eq. 20, x_w is a regular sinusoidal water wave, which is a function of time. Initial conditions given in Eq. 21 represent the situation where the float is partially submerged at the crest of the wave form at t =0 seconds.

$$x_w=\frac{H}{2}\cos\left(\frac{2\pi}{T}t\right) \tag{20}$$

$$\theta(0)=\frac{H}{2R_m},\quad \dot{\theta}(0)=0 \tag{21}$$

It is noted here that the most desirable condition of float submergence is when the float is always partially submerged during motion from the viewpoint of increasing the energy gain and prolonging the life of the device (Matsuura 2006). Computational results presented in this paper are only for those cases of wave heights and wave periods where the device of given dimensions always heaves in the partially submerged condition.

EFFECT OF ADDED MASS FORCE AND DRAG FORCE

In this section, the effects of the added mass and drag forces on the behavior of the float motion, power output and the tensile force in the wire are discussed. The calculated results of the previous model where these opposing forces were not considered are compared with that of the present model. For calculation, the following data was used; mass of the float as 10367 kg, mass of counterweight as 4571 kg, radius of the driving pulley as 0.14m, float height as 3m, float diameter as 2m, gear ratio as 10, voltage constant as 0.135V/rpm, torque constant as 1.2838N.m/A, internal resistance as 0.26 Ohm, float submergence ratio as 0.6, viscous damping coefficient as 150 N.s/m, C_d as 1.0, C_m as 1.0. In the following figures, the curves with C_d and C_m equal to zero represent the results obtained from the previous model.

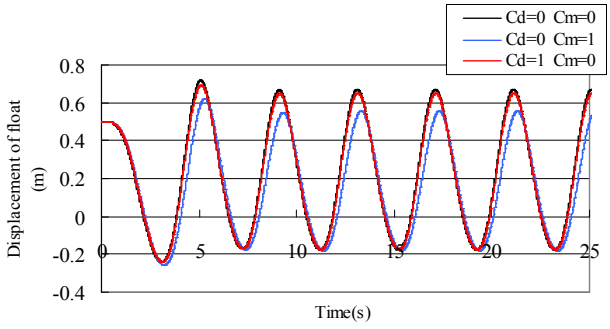

Fig. 4 Time series of the vertical displacement of float

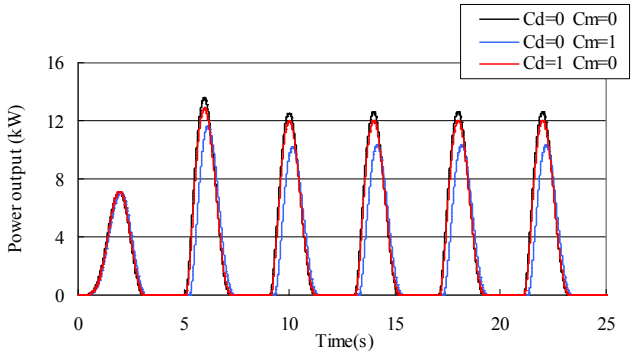

Fig. 5 Time series of the output power

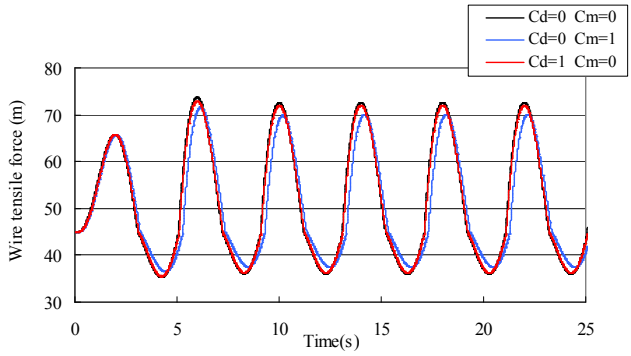

Fig. 6 Time series of the wire tensile force

Fig.4 shows that the amplitude of the float's displacement decreases only slightly due to the drag force, whereas the effect of the added mass is more prominent causing a greater reduction in the amplitude. It is also evident from the figure that a certain time lag occurs due to the added mass force. As a result, the energy gain as well as the wire tensile force is less when these opposing forces are considered as shown in Fig. 5 and Fig. 6. But for high values of the damping coefficient, the effects of the added mass and drag forces are found to be less pronounced and become insignificant beyond 500N.m/s for the given dimensions of the system.

VALIDATION OF THE MODEL

Experimental Setup

Experiments were conducted in an artificial wave tank at the Research and Development Center of Mitsubishi Heavy Industries LTD, Nagasaki, Japan. The wave tank used was 3.2 m deep, 30m wide and had an effective length of 160 m. At one side of the longitudinal direction was a wave maker and the model was set at the opposite side so that the float received waves directly. Fig. 7 indicates the model set in the wave tank. Floats were supported by idler pulleys mounted at an intermediate position of the beam supported by a vertical column. The experimental apparatus consisted of two pairs of floats and counterweights with the dimensions specified in Table 1. The shafts rotate with the same speed everywhere but individual torques are accumulated at points where they are connected to the driving pulleys. Regular waves were produced and the clutch was turned on at some proper time when the wave crest reached the floats. The water level, displacements of float, wire tensile force, torque, etc. were simultaneously measured. Wave conditions of wave period and wave heights for which experiments were performed are as follows: 1.8s/0.32m, 2.0s/0.25m, 3.0s/0.14m, 3.5s/0.24m, 4.0s/0.27m, 4.5s/0.15m and 5.0s/0.10m.

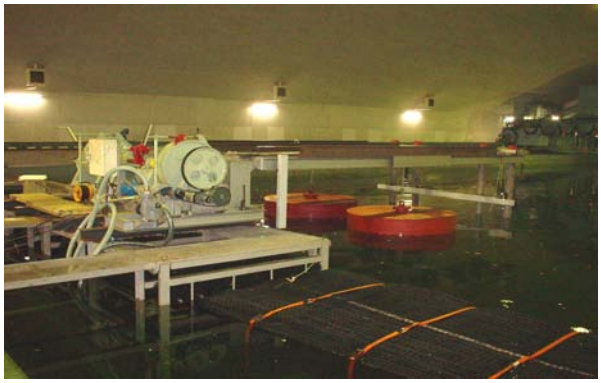

Fig. 7 Experimental setup

Table 1. Dimensions for experiment

Float	Density (kg/m^3)	745.7
	Height (m)	0.7
	Diameter (m)	2
	Submergence ratio	0.5714
	Mass (kg)	1680
Counterweight	Mass (kg)	150
Driving Pulley	Radius (m)	0.18
Gearbox	Gear ratio	41.36

Table 2. Experimental conditions for significant energy conversion

Experiment No.	Wave Height	Time Period	Average Energy conversion rate
	H(m)	T(s)	(Σwire tension*float speed*dt)/time(W)
1	0.27	4	80
2	0.24	3.5	60

Results of Experiment

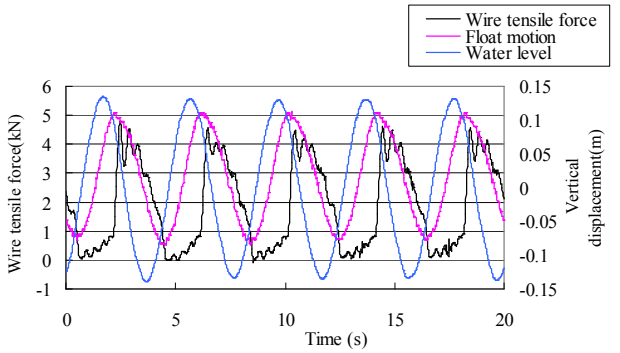

(a) Experiment No.1

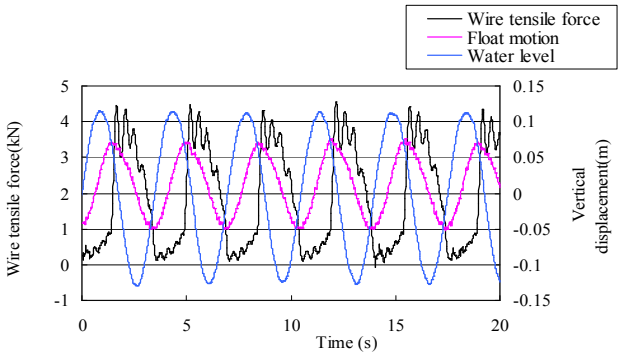

(b) Experiment No.2

Fig. 8 Time series of wire tensile force and float motion

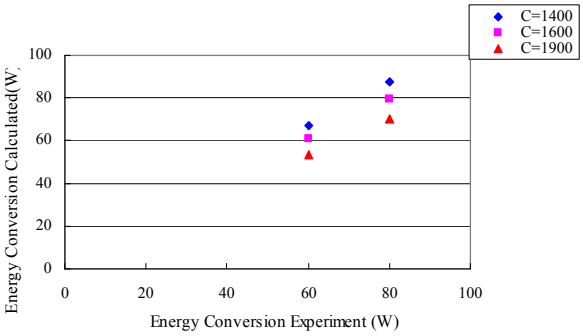

Fig. 9 Determination of damping coefficient C

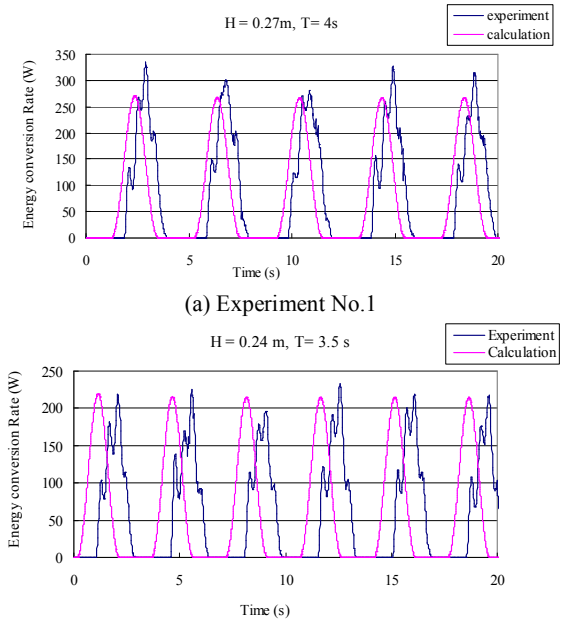

(a) Experiment No.1

(b) Experiment No.2

Fig. 10 Time series of energy conversion rate

In experiments with wave period shorter than 3 seconds, the device could not convert energy significantly due to the large pitching motion of the floats. However at wave conditions 3.5s/0.24m and 4.0s/0.27m, significant power output was observed on account of higher amplitude of heaving of the float. Behaviors of wire tensile force and float displacement during experiments are given in Fig. 8. It is found that the wire tensile force becomes nonzero immediately after the float displacement reached its peak and zero when the float is at the bottom. The value of the viscous damping coefficient, *C*, was determined by comparing the energy conversion rate data with the calculated values. The energy conversion rate obtained as the product of the tensile force and the speed of the float descent is basically a measure of the work performed by the tensile force in the cable in rotating the driving pulley. From Fig. 9, the value of *C* is approximately 1600N.m/s. Comparison between the experimental and computational values of energy conversion rate presented in Fig. 10 shows that they are relatively in good agreement. Thus, we can conclude that the current dynamics model is capable of simulating the physical model relatively accurately.

BEHAVIOUR OF ENERGY GAIN, TENSILE FORCE AND TORQUE AT DIFFERENT WAVE CONDITIONS

Using the refined model, the energy gain, maximum wire tensile force

Table 3. Calculation conditions

Physical Quantities	Values
Specific gravity of the float	1
Submerged height ratio	0.6
Mass of float (t)	21.21
Mass of counterweight (t)	8.16
Radius of driving pulley (m)	0.28
Viscous damping coefficient (N.s/m)	567
Gear ratio	20
Induced voltage coefficient (V/rpm)	0.135
Torque constant (N.m/A)	1.284
Internal resistance (Ohm)	0.26
Diameter of float (m)	3
Height of float (m)	3
Density of sea water (kg/m^3)	1025
Gravitational acceleration (m/s^2)	9.81

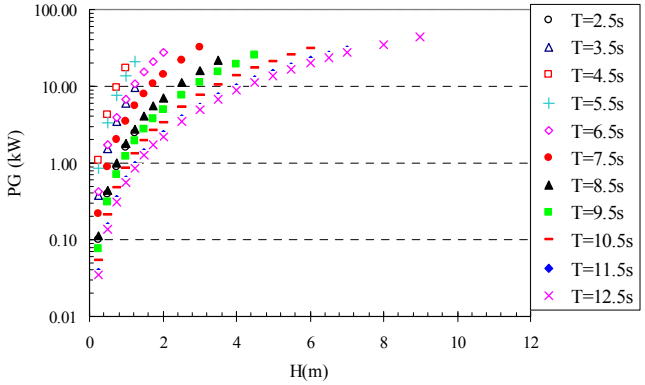

Fig. 11 Obtainable energy gain for different wave heights and periods

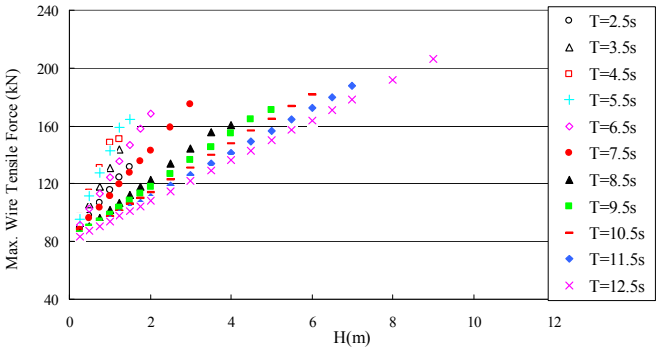

Fig. 12 Maximum wire tensile force for different wave heights and periods

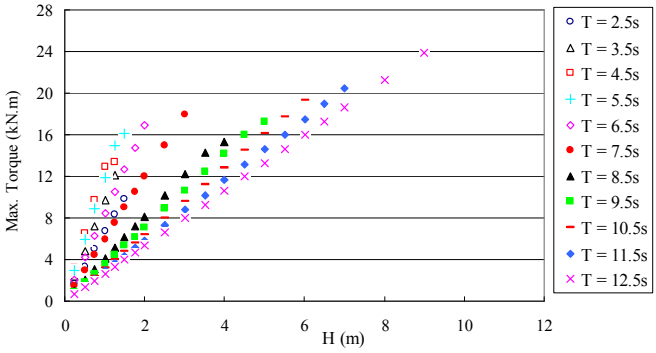

Fig. 13 Maximum torque for different wave heights and periods

and maximum torque have been calculated for the system dimensions specified in Table 3 at different wave heights and wave periods, and the results are presented as Figs. 11~13 respectively. The added mass and the drag coefficients are each set to 1.0. The energy gain is found to increase with the increase in the wave height for given time period as shown in Fig. 11, the vertical axis of which has been plotted in logarithmic scale. On the otherhand, for a given wave height, it increases gradually with the time period and peaks at around 5 seconds for the given dimensions and then decreases with a further increase in the time period of the wave. This is due to the resonance phenomenon which is discussed in the next section (see Table 4). From Fig. 12, maximum value of the wire tensile force is found to increase proportionally with the wave height starting from the weight of the counterweight. The increasing rate falls with increase in the wave period, which corresponds to the slow up/down motion of the float and counterweight. Maximum torque also increases proportionally with wave height with a falling rate for longer wave periods as shown in Fig. 13.

RESONANCE PHENONMENON

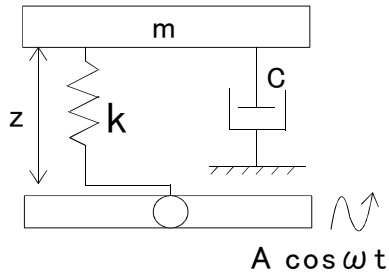

Fig. 14 Schematic indication of the relation between the wave force and float motion.

The resonant heaving motion of the float can be utilized to enhance the energy gain. Prototypes for the model can be designed so that the natural frequency of the system matches the dominant wave frequency at the local sea. This is particularly convenient for this system as it can be achieved by changing only the float and counterweight dimensions.
Fig. 14 indicates a mass-spring-dashpot system representing the physical phenomenon where Z is the displacement of spring, k is the spring constant, c is the damping coefficient and m is the system mass. The displacement of spring is the relative displacement between the float and water level given as Eq. 22.

$$z = R_m\theta - x_w \tag{22}$$

Therefore,

$$\theta = (z + x_w)/R_m \tag{23}$$

Using Eq. 23 in Eq. 16, and replacing the added mass term by M_{added} we obtain,

$$\left(\frac{I}{R_m} + (M_c + M_f + M_{addad})R_m\right)\frac{d^2}{dt^2}\left(\frac{z}{R_m} + \frac{x_w}{R_m}\right) + \frac{1}{R_m}\left(C + \frac{G^2}{r}k_\tau k_e\right) \tag{24}$$

$$\frac{d}{dt}\left(\frac{z}{R_m} + \frac{x_w}{R_m}\right) + \frac{\rho g\pi}{4}d_f^2 R_m\left(\frac{z}{R_m} + \frac{x_w}{R_m}\right) = \frac{\rho g\pi}{4}d_f^2 x_w$$

After substituting $x_w = A\cos\omega t$ in Eq. 24 and simplifying, we get

$$\left\{\frac{I}{R_m^2} + M_c + M_f + M_{added}\right\}\frac{d^2z}{dt^2} + \frac{1}{R_m^2}\left(C + \frac{G^2}{r}k_\tau k_e\right)\frac{dz}{dt} + \frac{\rho g\pi d_f^2}{4}z = \tag{25}$$

$$\left\{\frac{I}{R_m^2} + (M_c + M_f + M_{addded})\right\}A\omega^2\cos\omega t + \frac{\left(C + \frac{G^2k_\tau k_e}{r}\right)}{R_m^2}A\omega\sin\omega t$$

which can be expressed as

$$\left\{\frac{I}{R_m^2} + M_c + M_f + M_{added}\right\}\frac{d^2z}{dt^2} + \frac{1}{R_m^2}\left(C + \frac{G^2}{r}k_\tau k_e\right)\frac{dz}{dt} + \frac{\rho g\pi d_f^2}{4}z = \tag{26}$$

$$\sqrt{\left\{\left(\frac{I}{R_m^2} + M_c + M_f + M_{added}\right)A\omega^2\right\}^2 + \left\{\frac{A\omega\left(C + \frac{G^2k_\tau k_e}{r}\right)}{R_m^2}\right\}^2}\sin(\omega t - \varphi)$$

The contribution of the drag force is quite small as discussed in the previous section on the effects of the added mass and drag force (also referenced from Sarpkaya 1981). Although the amplitude of the oscillation will decrease slightly due to this force, it has not been considered in the equations describing the resonance phenomenon as it makes the analysis very complex. However, the authors will consider it in the future analysis. Also, to avoid complexity in calculation, the added mass is assumed to be equal to the mass of water displaced at stationary floating condition.
From Eq. 26, the natural frequency of the system, ω_n and the damping factor, ξ can be written as Eqs. 27~28 respectively.

$$\omega_n = \sqrt{\frac{k}{m}} = \sqrt{\frac{\rho g\pi d_f^2}{4\left\{\frac{I}{R_m^2} + (M_c + M_f + M_{added})\right\}}} \tag{27}$$

$$\zeta = \frac{C}{2\sqrt{mk}} = \frac{\left(C + \frac{G^2k_\tau k_e}{r}\right)}{2\sqrt{\left\{I + (M_c + M_f + M_{addad})R_m^2\right\}\left(\frac{\rho g\pi d_f^2}{4}\right)}} \tag{28}$$

Also,

$$\frac{x_0}{x_{stat}} = \frac{1}{\sqrt{\left(1 - \frac{\omega^2}{\omega_n^2}\right)^2 + \left(2\zeta\frac{\omega}{\omega_n}\right)^2}} \tag{29}$$

where, x_0: amplitude of forced oscillation and x_{stat}: displacement of the float at static free condition.

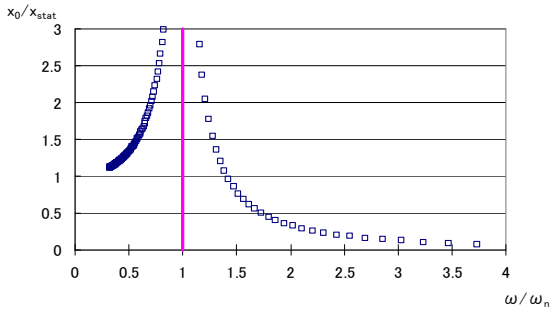

Fig. 15 The displacement-resonance curve

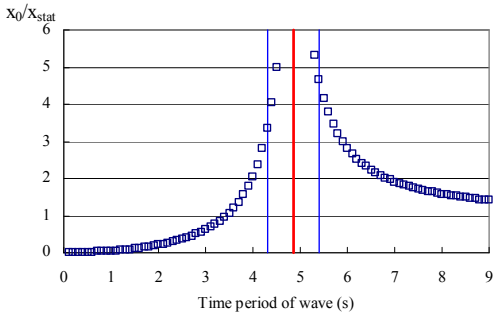

Fig. 16 Determination of the resonance period

Table 4. Time averaged energy gain (kW) indicating the maximum value at resonance

H(m) \ T(s)	2.5	3.5	4.5	5.5	6.5	7.5	8.5	9.5	10.5	11.5	12.5
10											
9											44.85
8											35.43
7										29.28	27.13
6.5										25.24	23.39
6									30.60	21.51	19.93
5.5									25.71	18.07	16.75
5									21.25	14.94	13.84
4.5								25.03	17.21	12.10	11.21
4								19.78	13.60	9.56	8.86
3.5							21.88	15.14	10.41	7.32	6.78
3						31.92	16.07	11.12	7.65	5.38	4.98
2.5						22.17	11.16	7.73	5.31	3.73	3.46
2					27.59	14.19	7.14	4.94	3.40	2.39	2.21
1.75					21.12	10.86	5.47	3.79	2.60	1.83	1.70
1.5					15.52	7.98	4.02	2.78	1.91	1.34	1.25
1.25	2.46	9.54		21.27	10.78	5.54	2.79	1.93	1.33	0.93	0.87
1	1.57	6.11	17.07	13.61	6.90	3.55	1.79	1.24	0.85	0.60	0.55
0.75	0.89	3.44	9.60	7.66	3.88	2.00	1.00	0.70	0.48	0.34	0.31
0.5	0.39	1.53	4.27	3.40	1.72	0.89	0.45	0.31	0.21	0.15	0.14
0.25	0.10	0.38	1.07	0.85	0.43	0.22	0.11	0.08	0.05	0.04	0.03

Dimensions of the system and other physical quantities used in this calculation are given in Table 3 of the previous section. As shown in Fig. 15, the displacement ratio becomes maximum when the frequency of the excitation force, wave force in this case, equals the natural frequency of the system. From Eqs.27~28, the resonance period and damping factor for the given system dimensions were found to be around 4.8 seconds shown graphically in Fig. 16, and 0.05 respectively. Therefore the system is underdamped and will oscillate. Table 4 demonstrates the energy gain of the device for different wave heights and wave periods. It is found from the table that the energy gain increases gradually with the wave period and peaks at around the resonance period indicated by the highlighted cells in Table 4,and decreases with further increase in the time period. To enhance efficiency, it is important to design the prototypes of the device so that the natural frequency of the system matches the dominant wave frequency at the local sea. Blank cells indicate the wave conditions where the float is not always partially submerged and are not considered in the calculation.

CONCLUSIONS

A refined mechanical dynamics model was presented for the float-type wave energy conversion system considering the drag and added mass forces. Experimental results of the energy conversion rate were found to be in fairly good agreement to the calculated values of the proposed model. Analysis of the resonance phenomenon showed that in order to enhance the energy conversion, the system components may be designed so that the natural frequency of the system matches dominant wave frequency at the location site. Wire tensile force and the driving pulley torque were found to vary linearly with the wave height and wave period.

REFERENCES

Evans, DV(1982),"Wave Power Absorption Within a Resonant Harbor", *Proc 2nd Int Symp On Wave Energy Utilization*, Trendheim, pp 371-378.

Folley, M, Whittaker, T and Osterried, M (2004), " The Oscillating Wave Surge Converter", *Proc 14th Int Offshore and Polar Eng Conf*, Toulon, pp 189-193,CD-ROM.

Hadano, K, Saito, T, Kawano, S, Hashida, M, and Ozaki, T (1998)."A Proposal for Multi-Floats Type Wave Energy Conversion System," *Proc 8th Int Offshore and Polar Eng Conf*, Montreal, pp 100-105.

Hadano, K, Nakano, K, Taneura, K, Ohgi, K, and Koirala, P (2002). "On the Occurred Electric Power," *Proc Techno-Ocean 2002, Int Symp*, CD-ROM.

Hadano, K, Taneura, K, Saito, T, and Nakano, K (2004). " Evaluation of Energy Obtained by Float-Type wave Energy Generation System." *Proc 14th Int Offshore and Polar Eng Conf*, Toulon, pp 246-252,CD-ROM.

Hadano, K, Hashida, M, and Sato, M (2001)."Experiment on the Energy Gain of Floats-Type Wave Generator," *Proc 11th Int Offshore and Polar Eng Conf*, Stavanger, pp 638-645.

Hadano, K, Hashida, M, and Sato, M (2002). "An Attempt to Make High Performance Wave Energy System," *Proc 12th Int Offshore and Polar Eng Conf*, Kitakyshu, pp 556-561.

Hadano, K, Taneura, K, Watanabe, M, Saito, T, Nakano, K, Masami, M (2006)."Mechanics of the Float Type Wave Energy conversion." *Proc 16th Int Offshore and Polar Eng. Conf.*, San Francisco, pp 430-436,CD-ROM.

Hooft, JP, Advanced Dynamics of Marine Structures, John Wiley & Sons, 1982

Malm, O and Reiten, A(1985),"Wave Power Absorption by an Oscillating Water Column in a Channel", Journal of Fluid Mechanics,158, pp 153-175.

Nagai, N, Sato, K, and Sugawara, K (2002). "Technical Note of the Port and Airport Research Institute No.1017." *Independent Administrative Institution Port and Airport Research Institute*, Japan, pp 79-331(in Japanese).

Pontes, MT, Falcao, A (2001), "*Ocean Energies: Resources and Utilization"*, World Energy Council, 18th Congress, Buenos Aires.

Sarpkaya, T, Isaacson, M, Mechanics of Wave Forces on Offshore Structures, Van Nostrand Reinhold Company Inc., 1981

Suzuki, M, Kuboki, T, Arakawa, C and Nagata, S (2006), " Numerical Analysis on Optimal Profile of Floating Device with OWC Type Wave Energy Converter", *Proc 16th Int Offshore and Polar Eng Conf*, San Francisco, pp 466-470,CD-ROM.

World Energy Outlook 2005, www.Worldenergyoutlook.org

World Energy Council, http://www.worldenergy.org